Thermodynamics of novel charged dilaton black holes in gravity's rainbow

M. Dehghani

Department of Physics, Razi University, Kermanshah, Iran

A R T I C L E   I N F O

A B S T R A C T

In the present work, we have studied the thermodynamical properties of black holes arising as the solutions of the four-dimensional dilaton gravity coupled to Maxwell's electrodynamics in gravity's rainbow. This theory allows three classes of asymptotically non-flat and non-AdS black hole solutions. We showed that the self-interacting scalar function, as the solution to the scalar field equation, can be written as the linear combination of three Liouville-type potentials. The thermodynamical quantities are identified and in particular, a generalized Smarr formula is derived. It is shown that, although the thermodynamic quantities are affected by the rainbow functions, the validity of the black hole thermodynamical first law is supported. The thermodynamic stability of the solutions have been analyzed through the black hole heat capacity. We have shown that, even in the presence of the rainbow functions, the black holes can be locally stable in the sense that there exists a range of the horizon radiuses for which the heat capacity is positive.

1. Introduction

One of the more outstanding problems in the context of theoretical physics is to combine the gravity with the quantum mechanics and to construct the theory of quantum gravity. Despite the attempts made through the string theory [1,2], loop quantum gravity [3], space time foam [4], Horava–Lifshitz gravity [5], non-commutative geometry [6] and other approaches there is currently no complete theory of quantum gravity and this problem is still open. A common feature of almost all of these alternative approaches is a strong interest on the modification of the usual energy-momentum dispersion relation at the Planck-scale regime [7,8]. It seems that this modification plays an important role in establishing a full theory of quantum gravity, but it leads to the violation of Lorentz invariance, as the most fundamental symmetry in the universe. One of the approaches to overcome this problem is the doubly or deformed special relativity [9,10]. The doubly special relativity, as a modified formalism of special relativity, has been proposed to make the modified dispersion relation Lorentz invariant [11–13]. In the high energy formalism of the special relativity, known as the doubly special relativity, the speed of light and the Planck energy are two Lorentz invariant quantities. Also, the Planck energy and the speed of light are the upper bounds of

the energy and velocity that a particle can attain [14]. This theory is accomplished based on a nonlinear Lorentz transformation in the momentum space in such a way that the energy-momentum relation appears with the corrections in the order of the Planck length and the Planck-scale corrected dispersion relation preserves a deformed Lorentz symmetry [11,15].

The doubly special relativity has now been extended to the curved space times and a doubly general relativity or gravity's rainbow has been proposed by Magueijo and Smolin [16,17]. In the rainbow gravity theory, the geometry of space time depends on the energy of the test particle. Thus, it seems different for the particles having different amounts of energy and the energy dependent metrics form a rainbow of metrics. This is why the double general relativity is named as gravity's rainbow. The modified dispersion relation can be written in the following general form [18,19]

$$E^2 f^2(\varepsilon) - p^2 g^2(\varepsilon) = m^2, \tag{1.1}$$

where, $\varepsilon = E/E_P$, E_P is the Planck-scale energy, E is the energy of the test particle and the functions $f(\varepsilon)$ and $g(\varepsilon)$ are known as the rainbow functions. The rainbow functions are satisfied the following conditions

$$\lim_{\varepsilon \to 0} f(\varepsilon) = 1, \quad \text{and} \quad \lim_{\varepsilon \to 0} g(\varepsilon) = 1. \tag{1.2}$$

E-mail address: m.dehghani@razi.ac.ir.

By these requirements one is able to reproduce the standard dispersion relation in the limit of $\varepsilon \to 0$. It must be noted that the functional form of the rainbow functions are not unique and there are several expressions for them which are correspond to different phenomenological motivations. Some of the proposed models for the temporal and spatial rainbow functions are as follows [20,21]

$$f(\varepsilon) = 1, \quad \text{and} \quad g(\varepsilon) = \sqrt{1 - \eta \varepsilon^n}, \tag{1.3}$$

$$f(\varepsilon) = \frac{e^{\xi \varepsilon} - 1}{\xi \varepsilon}, \quad \text{and} \quad g(\varepsilon) = 1, \tag{1.4}$$

$$f(\varepsilon) = g(\varepsilon) = \frac{1}{1 - \lambda \varepsilon}, \tag{1.5}$$

where, η, n, ξ and λ, known as the rainbow parameters, are dimensionless constants of the order of unity.

Nowadays, gravity's rainbow, in which the quantum gravitational effects are taken into account, has attracted a lot of interest and many papers have been appeared in which the physical properties of the black holes are investigated in the presence of rainbow functions. Thermodynamics and phase transition of the modified Schwarzschild black holes via gravity's rainbow are studied in refs. [19,22]. Thermal stability of nonlinearly charged BTZ and four-dimensional rainbow black holes has been analyzed in refs. [23,24]. The effects of rainbow functions on the rotating BTZ black holes are the subject of ref. [25]. Thermodynamics of Gauss–Bonnet black holes in rainbow gravity has been discussed in refs. [26,27]. Also, thermodynamics and stability of the black holes have been studied in the context of massive gravity's rainbow by Hendi et al. [28,29]. Study of the physics in the energy dependent space times has provided many interesting results such as: black hole remnant [30,31], nonsingular universe [32], etc.

Thermodynamics and thermal stability of charged dilatonic BTZ black holes in gravity's rainbow have been studied in ref. [18] in the presence of Coulomb and modified Coulomb fields, separately. The impacts of thermal fluctuations, as a quantum gravitational phenomenon, on the thermodynamic phase transition of rainbow dilaton black holes have been investigated in my last work [33]. Here, I tend to extend my previous works to the case of electrically charged four-dimensional dilaton black holes. The main object is to obtain the new exact black hole solutions to the Einstein–Maxwell-dilaton theory in rainbow gravity and to investigate the thermodynamic proprieties as well as the thermal stability or phase transition of the new charged rainbow black holes.

The plan of this paper is organized as follows: Sec. 2 is devoted to solving the coupled gravitational, electromagnetic and scalar field equations in an energy dependent space time. The solution to the scalar field equation has been written as the linear combination of three Liouville-type potentials. Three new classes of spherically symmetric charged dilaton black hole solutions, with the non flat and non A(dS) asymptotic behavior, have been obtained. The thermodynamic properties of new rainbow black holes have been studied in Sec. 3. Through a Smarr-type mass formula in which the black hole mass has been written as a function of black hole charge Q and black hole entropy S, it has been found that the first law of black hole thermodynamics is still valid. In Sec. 4, making use of the canonical ensemble method and regarding the signature of the black hole heat capacity, a thermal stability analysis has been performed. The points of type-1 and type-2 phase transitions as well as the ranges of the black hole horizon radii at which the black holes are locally stable are determined, exactly. Some concluding remarks and discussions are summarized in Sec. 5.

2. The field equations in gravity's rainbow

The action of four-dimensional Einstein–Maxwell-dilaton gravity theory can be written in the following general form [24,34]

$$I = \frac{1}{16\pi} \int \sqrt{-g} d^4 x \left[\mathcal{R} - V(\phi) - 2(\nabla \phi)^2 - \mathcal{F} e^{-2\alpha\phi} \right]. \tag{2.1}$$

Here, $\mathcal{R}$ is the Ricci scalar, ϕ is a scalar field coupled to itself via the functional form $V(\phi)$ and the last term denotes the coupled scalar-electromagnetic lagrangian. The parameter α is the scalar-electromagnetic coupling constant and $\mathcal{F} = F^{\mu\nu} F_{\mu\nu}$ being the Maxwell invariant, $F_{\mu\nu} = \partial_\mu A_\nu - \partial_\nu A_\mu$ is the Maxwell's electromagnetic tensor and A_μ denotes the electromagnetic potential. By varying the action (2.1) with respect to electromagnetic, gravitational and scalar fields, we get the related field equations which are in the following forms

$$\nabla_\mu \left[e^{-2\alpha\phi} F^{\mu\nu} \right] = 0, \tag{2.2}$$

$$\mathcal{R}_{\mu\nu} - \frac{1}{2} g_{\mu\nu} V(\phi) = 2\nabla_\mu \phi \nabla_\nu \phi + e^{-2\alpha\phi} \left(2 F_{\mu\rho} F_\nu{}^\rho - \frac{1}{2} \mathcal{F} g_{\mu\nu} \right), \tag{2.3}$$

$$4 \Box \phi = \frac{dV(\phi)}{d\phi} - 2\alpha \mathcal{F} e^{-2\alpha\phi}, \quad \phi = \phi(r). \tag{2.4}$$

We would like to solve the above field equations in a four-dimensional spherically symmetric geometry with the following line element [18,33]

$$ds^2 = -\frac{U(r)}{f^2(\varepsilon)} dt^2 + \frac{1}{g^2(\varepsilon)} \left[\frac{1}{U(r)} dr^2 + r^2 R^2(r)(d\theta^2 + \sin^2\theta d\varphi^2) \right]. \tag{2.5}$$

It must be noted that the only nonvanishing component of electromagnetic field is F_{tr}. Assuming as a function of r, $\mathcal{F} = -2 f^2(\varepsilon) g^2(\varepsilon)(F_{tr}(r))^2$. In order to obtain the metric function $U(r)$, we use Eq. (2.5) in the gravitational field equations (2.3). It leads to the following differential equations

$$e_{tt} = \frac{g^2(\varepsilon)}{2} \left[U''(r) + 2 \left(\frac{1}{r} + \frac{R'(r)}{R(r)} \right) U'(r) \right] + \frac{1}{2} V(\phi) - f^2(\varepsilon) g^2(\varepsilon) F_{tr}^2 e^{-2\alpha\phi} = 0, \tag{2.6}$$

$$e_{rr} = e_{tt} + 2 \left(\frac{R''(r)}{R(r)} + \frac{2R'(r)}{rR(r)} + (\phi'(r))^2 \right) U(r) = 0, \tag{2.7}$$

$$e_{\theta\theta} = e_{\varphi\varphi} = \left(\frac{1}{r} + \frac{R'(r)}{R(r)} \right) U'(r)$$
$$+ \left(\frac{1}{r^2} + \frac{R''(r)}{R(r)} + \frac{4R'(r)}{rR(r)} + \frac{R'^2(r)}{R^2(r)} \right) U(r)$$
$$- \frac{1}{r^2 R^2(r)} + \frac{1}{2g^2(\varepsilon)} \left[V(\phi) + 2 f^2(\varepsilon) g^2(\varepsilon) F_{tr}^2 e^{-2\alpha\phi} \right]$$
$$= 0, \tag{2.8}$$

for the tt, rr and $\theta\theta$ $(\varphi\varphi)$ components, respectively. Regarding Eqs. (2.6) and (2.7) we have

$$\frac{R''(r)}{R(r)} + \frac{2}{r} \frac{R'(r)}{R(r)} + \phi'^2(r) = 0. \tag{2.9}$$

The differential equation (2.9) can be rewritten in the following form

$$\frac{2}{r}\frac{d}{dr}\ln R(r) + \frac{d^2}{dr^2}\ln R(r) + \left(\frac{d}{dr}\ln R(r)\right)^2 + (\phi'(r))^2 = 0. \quad (2.10)$$

From Eq. (2.10), one can argue that $R(r)$ must be an exponential function of $\phi(r)$. Thus, we can use exponential solution of the form $R(r) = e^{\beta\phi}$ in Eq. (2.9), and show that $\phi = \phi(r)$ satisfies the following differential equation

$$\beta\phi'' + (1+\beta^2)\phi'^2 + \frac{2\beta}{r}\phi' = 0. \quad (2.11)$$

It is easy to write the solution of (2.11) in terms of a positive constant b as

$$\phi(r) = \gamma \ln\left(\frac{b}{r}\right), \quad \text{with} \quad \gamma = \beta(1+\beta^2)^{-1}. \quad (2.12)$$

It must be mentioned that, a similar solution has been used previously for three- and four-dimensional charged and uncharged dilatonic black hole solutions [33,35–37].

Here, we are interested on studying the effects of the exponential solution (i.e. $R(r) = e^{\beta\phi}$) with both $\beta = \alpha$ and $\beta \neq \alpha$ on the thermodynamic behavior of the four-dimensional charged dilatonic black hole solutions. The case correspond to $\beta = \alpha$ has been studied by some authors [38,39]. Now, we proceed to solve the field equations, making use of the scalar fields given by Eq. (2.12).

Let us start with the electromagnetic field equation (2.2). Making use of these solutions together with Eqs. (2.2) and (2.5), one can show that $h(r) = A_\mu(r)\delta_0^\mu$, satisfies the following differential equation

$$r^{B-1}\left(rh'' + Bh'\right) = 0, \quad \text{with} \quad B = 2[1 + \gamma(\alpha - \beta)]. \quad (2.13)$$

The solution to the above differential equation can be written as

$$h(r) = \frac{q}{1-B}r^{1-B}, \quad \text{and} \quad F_{rt} = q\,r^{-B}, \quad (2.14)$$

where, q is an integration constant related to the charge of black hole. It must be noted that, in order to the potential $h(r)$ be physically reasonable (i.e. zero at infinity), $1 - B$ must be negative. It means that α and β must be chosen such that $2\gamma(\alpha - \beta) > -1$. The electric field (2.14) reduces to the inverse-square Coulomb's law for $\beta = \alpha$. In the case $\beta \neq \alpha$, Eq. (2.14) can be interpreted as the modified Coulomb's electric field and electric potential [34,37].

Now, making use of these solutions in Eqs. (2.4) and (2.8) we arrived at

$$\frac{dV(\phi)}{d\phi} - 2\beta V(\phi) + 4(\alpha - \beta)f^2(\varepsilon)g^2(\varepsilon)F_{tr}^2 e^{-2\alpha\phi} + \frac{4\beta g^2(\varepsilon)}{r^2 R^2}$$
$$= 0, \quad (2.15)$$

$$\frac{\gamma}{\beta r}\left(U' + \frac{1-2\beta\gamma}{r}U\right) - \frac{1}{r^2 R^2}$$
$$+ \frac{1}{2g^2(\varepsilon)}\left[V(\phi) + 2f^2(\varepsilon)g^2(\varepsilon)F_{tr}^2 e^{-2\alpha\phi}\right] = 0, \quad (2.16)$$

for the metric function $U(r)$ and $V(\phi)$, respectively. The solution to Eq. (2.15) can be written in the following form

$$V(\phi) = \begin{cases} 2\Lambda e^{2\theta\phi} + 2\Lambda_1 e^{2\theta_1\phi} + 2\Lambda_2 e^{2\theta_2\phi}, & \beta \neq 1, \\ 2(\Lambda + \lambda_1)e^{2\phi} + 2\lambda_2\phi e^{2\phi} + 2\lambda_3 e^{2(\alpha+2)\phi}, & \beta = 1, \end{cases}$$
$$(2.17)$$

where

$$\Lambda_1 = -\frac{q^2 f^2(\varepsilon)g^2(\varepsilon)\beta(\alpha-\beta)b^{-2B}}{(B-\alpha\gamma)(1+\beta^2)-\beta^2}, \quad \Lambda_2 = \frac{\beta^2 g^2(\varepsilon)}{b^2(\beta^2-1)},$$

$$\theta = \beta = \frac{1}{\theta_2}, \quad \theta_1 = \frac{B}{\gamma} - \alpha,$$

$$\lambda_1 = \frac{q^2 f^2(\varepsilon)g^2(\varepsilon)}{b^{2(\alpha+1)}}\cdot\frac{\alpha-1}{\alpha+1} = -\lambda_3, \quad \lambda_2 = -\frac{2g^2(\varepsilon)}{b^2}.$$

By requirement that, in the absence of the dilaton field (i.e. $\phi = 0$ or equivalently $\beta = 0 = \gamma$) the action (2.1) reduces to the action of Einstein–Maxwell gravity with cosmological constant, the condition $V(\phi = 0) = 2\Lambda = -6\ell^{-2}$ is fulfilled [40,41]. Also, Eq. (2.17) shows that the dilatonic potential can be written as the linear combination of three Liouville-type potentials.

Making use of Eq. (2.17) in Eq. (2.16), after some manipulations, we obtained the metric function $U(r)$ as

$$U(r) = \begin{cases} \frac{-m}{r^{1-2\beta\gamma}} + \frac{1+\beta^2}{1-\beta^2}\left(\frac{r}{b}\right)^{2\beta\gamma} + \frac{\Lambda b^2(1+\beta^2)^2}{g^2(\varepsilon)(\beta^2-3)}\left(\frac{r}{b}\right)^{2-2\beta\gamma} \\ \quad + \frac{q^2 f^2(\varepsilon)(1+\beta^2)P(\beta)}{(B-1)b^{2(B-1)}}\left(\frac{b}{r}\right)^{2(B-1-\alpha\gamma)}, \quad \beta \neq 1,\sqrt{3}, \quad \text{(a)} \\ -mr^{\frac{1}{2}} - 2\left(\frac{r}{b}\right)^{\frac{3}{2}} - \frac{4\Lambda b^2}{g^2(\varepsilon)}\left(\frac{r}{b}\right)^{\frac{1}{2}}\ln\left(\frac{r}{L}\right) + \frac{8q^2 f^2(\varepsilon)P(\beta=\sqrt{3})}{(\sqrt{3}\alpha-1)b^{\sqrt{3}-1}} \\ \quad \times \left(\frac{b}{r}\right)^{\frac{1}{2}(\sqrt{3}\alpha-2)}, \quad \beta = \sqrt{3}, \alpha > \frac{1}{\sqrt{3}}, \quad \text{(b)} \\ -m + 2\left[2 - (\Lambda + \lambda_1)\frac{b^2}{g^2(\varepsilon)} + \ln\left(\frac{b}{r}\right)\right]\left(\frac{r}{b}\right) \\ \quad + \frac{4q^2 f^2(\varepsilon)}{\alpha(\alpha+1)b^{2\alpha}}\left(\frac{b}{r}\right)^{\alpha}, \quad \beta = 1, \alpha > 0 \quad \text{(c)}, \end{cases}$$
$$(2.18)$$

where, L is a dimensional constant, m is the constant of integration related to the black hole mass which will be determined later and

$$P(\beta) = 1 + \frac{\beta(\beta-\alpha)}{(B-\alpha\gamma)(1+\beta^2)-\beta^2}.$$

It is notable that, in the infrared limit, the solutions are just the dilatonic black holes obtained in ref. [34] and in the absence of dilaton field (i.e. $\beta = 0 = \gamma$), the metric function $U(r)$ coincides with that of Reissner–Nordström-A(dS).

In order to examine the existence and the number of the real roots of the new metric functions, we just obtained, the plots of the metric functions (2.18) versus r, in terms of different values of the rainbow functions $f(\varepsilon)$ and $g(\varepsilon)$, are shown in Figs. 1–6 for $\beta = \alpha$ and $\beta \neq \alpha$, cases, separately. It is notable that the plots show that two horizon, extreme and naked singularity black holes can occur provided that the parameters of the theory are fixed, properly.

Now, we look at the Ricci and Kretschmann scalars for considering the space–time singularities. It is a matter of calculation to show that the Ricci and Kretschmann scalars are finite for finite values of the radial component r. Also, we have

$$\lim_{r\to\infty}\mathcal{R} = 0, \quad \text{and} \quad \lim_{r\to 0}\mathcal{R} = \infty, \quad (2.19)$$

$$\lim_{r\to\infty}\mathcal{R}^{\mu\nu\rho\lambda}\mathcal{R}_{\mu\nu\rho\lambda} = 0, \quad \text{and} \quad \lim_{r\to 0}\mathcal{R}^{\mu\nu\rho\lambda}\mathcal{R}_{\mu\nu\rho\lambda} = \infty. \quad (2.20)$$

Therefore, there is an essential (not coordinate) singularity located at $r = 0$. Together, the appearance of a singularity in the Ricci scalars and the existence of the horizons are sufficient to ensure the validity of the black hole solutions. Also, the asymptotic behavior of the solutions, just like the case of pure dilaton black hole solutions, are neither flat nor A(dS).

3. Thermodynamic quantities and thermodynamical first law

After the discoveries of Hawking et al., the black holes are considered as the thermodynamic systems with the well-defined thermodynamic properties such as entropy and temperature. In order
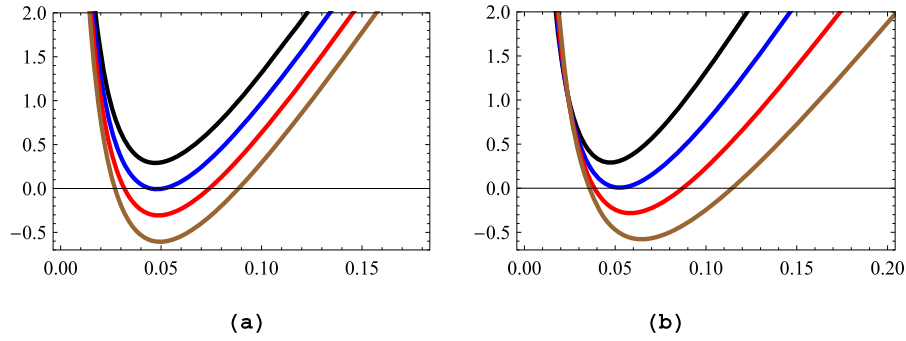
Fig. 1. $U(r)$ versus r for $Q = 0.5$, $M = 5$, $\Lambda = -3$, $b = 2$, $\alpha = \beta = 1.2$, Eq. (2.18)-a. (a): $g(\varepsilon) = 0.8$, $f(\varepsilon) = 1.02$ (black), 1.08 (blue), 1.14 (red), 1.2 (brown). (b): $f(\varepsilon) = 1.02$, $g(\varepsilon) = 0.8$ (black), 0.83 (blue), 0.86 (red), 0.89 (brown). (For interpretation of the colors in the figure(s), the reader is referred to the web version of this article.)
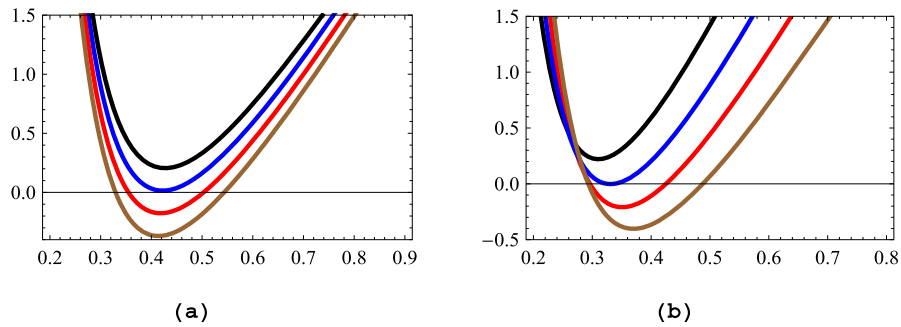

Fig. 2. $U(r)$ versus r for $Q = 0.5$, $M = 1.5$, $\Lambda = -3$, $b = 2$, $\alpha = 2$, $\beta = 0.5$, Eq. (2.18)-a. (a): $g(\varepsilon) = 0.8$, $f(\varepsilon) = 0.75$ (black), 0.8 (blue), 0.85 (red), 0.9 (brown). (b): $f(\varepsilon) = 1$, $g(\varepsilon) = 0.55$ (black), 0.6 (blue), 0.65 (red), 0.7 (brown).
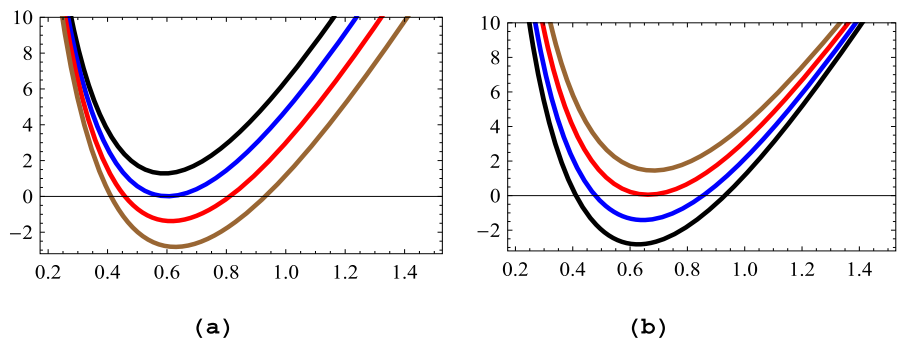

Fig. 3. $U(r)$ versus r for $Q = 5$, $M = 1.5$, $\Lambda = -3$, $b = 1.5$, $\beta = \sqrt{3}$ and $\alpha = \beta$, Eq. (2.18)-b. (a): $g(\varepsilon) = 0.75$ and $f(\varepsilon) = 0.2$ (black), 0.56 (blue), 0.95 (red), 1.35 (brown). (b): $f(\varepsilon) = 1.35$ and $g(\varepsilon) = 0.7$ (black), 0.708 (blue), 0.7166 (red), 0.725 (brown).
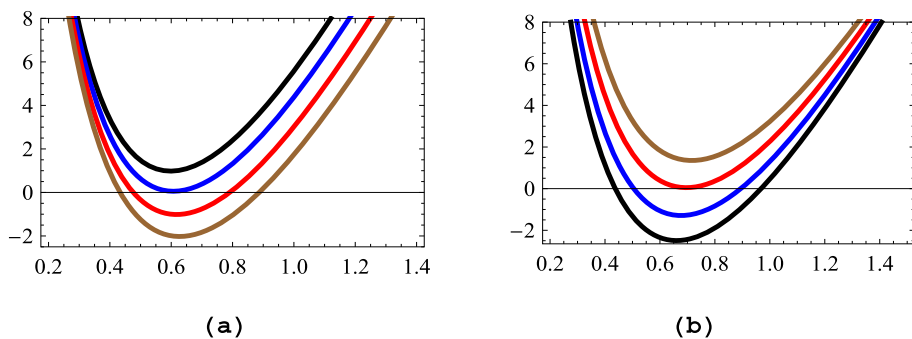

Fig. 4. $U(r)$ versus r for $Q = 5$, $M = 2.8$, $\Lambda = -3$, $b = 1.5$, $\alpha = 1.65$, $\beta = \sqrt{3}$ Eq. (2.18)-b. (a): $g(\varepsilon) = 0.7$, $f(\varepsilon) = 0.6$ (black), 0.74 (blue), 0.9 (red), 1.05 (brown). (b): $f(\varepsilon) = 1.3$, $g(\varepsilon) = 0.707$ (black), 0.714 (blue), 0.722 (red), 0.73 (brown).
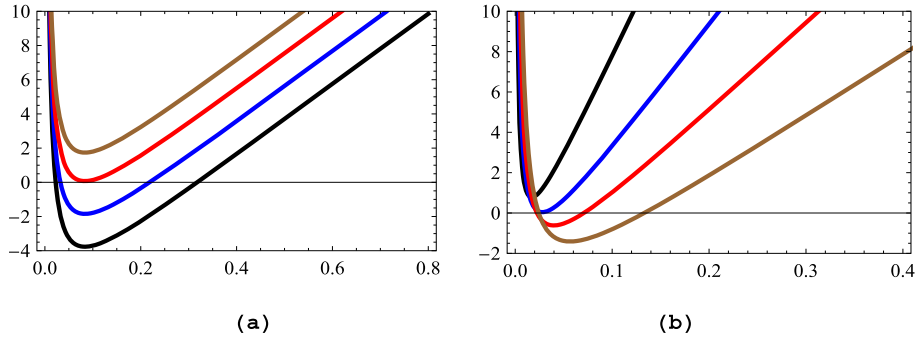
Fig. 5. $U(r)$ versus r for $Q = 0.5$, $M = 4$, $\Lambda = -3$, $b = 2$, $\alpha = \beta = 1$, Eq. (2.18-c). (a): $g(\varepsilon) = 0.8$, $f(\varepsilon) = 0.34$ (black), 0.6 (blue), 0.9 (red), 1.2 (brown). (b): $f(\varepsilon) = 1$, $g(\varepsilon) = 0.35$ (black), 0.45 (blue), 0.54 (red), 0.64 (brown).
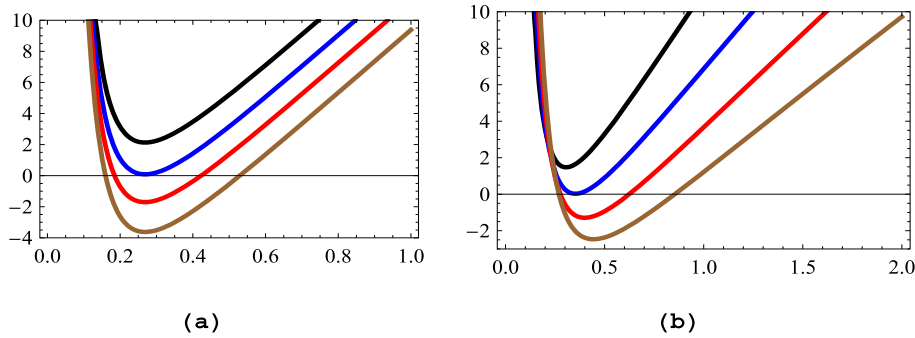

Fig. 6. $U(r)$ versus r for $Q = 0.5$, $M = 4$, $\Lambda = -3$, $b = 2$, $\alpha = 2.4$, $\beta = 1$, Eq. (2.18-c). (a): $g(\varepsilon) = 0.8$, $f(\varepsilon) = 1$ (black), 1.32 (blue), 1.6 (red), 1.9 (brown). (b): $f(\varepsilon) = 0.9$, $g(\varepsilon) = 0.9$ (black), 1.025 (blue), 1.15 (red), 1.27 (brown).

to check the satisfaction of the first law of black holes thermodynamics, we first compute the conserved and thermodynamic quantities. We drive the generalized Smarr mass formula and obtain the black hole mass as the function of the thermodynamical extensive parameters. Then, we compute the thermodynamical intensive parameters and show that the first law of black hole thermodynamics is satisfied.

The Hawking temperature associated to the black hole horizon, as an important thermodynamic quantity, can be expressed in terms of the black hole surface gravity, κ, that is $T = \frac{\kappa}{2\pi}$ from which one can show that

$$T = \frac{g(\varepsilon)}{4\pi f(\varepsilon) r_+}$$

$$\times \begin{cases} (1+\beta^2)\left[\frac{1}{1-\beta^2}\left(\frac{r_+}{b}\right)^{2\beta\gamma} - \frac{\Lambda b^2}{g^2(\varepsilon)}\left(\frac{b}{r_+}\right)^{2(\beta\gamma-1)} \right. \\ \left. - \frac{f^2(\varepsilon)q^2 P(\beta)}{b^{2(B-1)}}\left(\frac{b}{r_+}\right)^{2(B-1-\alpha\gamma)}\right], \quad \beta \neq \sqrt{3}, 1, \\ -2\left(\frac{b}{r_+}\right)^{-\frac{3}{2}} - \frac{4\Lambda b^2}{g^2(\varepsilon)}\left(\frac{b}{r_+}\right)^{-\frac{1}{2}} \\ - \frac{4f^2(\varepsilon)q^2 P(\beta=\sqrt{3})}{b^{\sqrt{3}\alpha-1}}\left(\frac{b}{r_+}\right)^{\frac{1}{2}(\sqrt{3}\alpha-2)}, \quad \beta = \sqrt{3}, \alpha > \frac{1}{\sqrt{3}}, \\ \frac{2r_+}{b}\left[1 - (\Lambda + \lambda_1)\frac{b^2}{g^2(\varepsilon)} + \ln\left(\frac{b}{r_+}\right)\right. \\ \left. - \left(\frac{f^2(\varepsilon)q^2}{b^{2\alpha}} - \frac{\lambda_1 b^2}{g^2(\varepsilon)}\right)\left(\frac{b}{r_+}\right)^{\alpha+1}\right], \quad \beta = 1, \alpha > 0. \end{cases}$$

(3.1)

Note that we have used the relation $U(r_+) = 0$ for eliminating the mass parameter, m, from the above relations. Also, it must be noted that the extreme black holes (i.e. black holes with zero temperature) may occur if the black hole charge q_{ext} and horizon radius, $r_+ = r_{ext}$, satisfy the following equations

$$q_{ext}^2 = \frac{b^{2(B-1)}}{f^2(\varepsilon)(1-\beta^2)P(\beta)}\left(\frac{r_{ext}}{b}\right)^B$$
$$\times \left[1 - \frac{\Lambda b^2(1-\beta^2)}{g^2(\varepsilon)}\left(\frac{r_{ext}}{b}\right)^{2(1-2\beta\gamma)}\right], \quad \beta \neq \sqrt{3}, 1, \quad (3.2)$$

$$q_{ext}^2 = \frac{b^{\sqrt{3}\alpha-1}}{2f^2(\varepsilon)P(\beta=\sqrt{3})}\left(\frac{r_{ext}}{b}\right)^{\frac{1}{2}(\sqrt{3}\alpha+1)}$$
$$\times \left[\frac{6b^2}{\ell^2 g^2(\varepsilon)}\left(\frac{b}{r_{ext}}\right) - 1\right], \quad \beta = \sqrt{3}, \alpha > \frac{1}{\sqrt{3}}, \quad (3.3)$$

$$q_{ext}^2 = \frac{(\alpha+1)\left[1 - \frac{\Lambda}{g^2(\varepsilon)}b^2 + \ln\left(\frac{b}{r_{ext}}\right)\right]b^{2\alpha}}{f^2(\varepsilon)\left[\alpha - 1 + 2\left(\frac{b}{r_{ext}}\right)^{\alpha+1}\right]}, \quad \beta = 1, \alpha > 0.$$

(3.4)

It is too difficult to obtain the real root(s) of the equation $T = 0$ given by Eqs. (3.2)–(3.4), analytically. In order to investigate the existence and the number of real roots of these equations, the plots of T versus r_+, are shown in Figs. 7–12 for different values of the rainbow functions $f(\varepsilon)$ and $g(\varepsilon)$. The plots of Figs. 7 and 8, which are related to the cases $\alpha = \beta$ and $\alpha \neq \beta$ in order, show that the equation $T = 0$ have a real root located at $r_+ = r_{ext}$, for the black holes with $\beta \neq 1$, $\sqrt{3}$. The un-physical black holes (i.e. the black holes with negative temperature) are occur if $r_+ < r_{ext}$ and the physical black holes having positive temperature can occur for $r_+ > r_{ext}$.

In the case $\beta = \sqrt{3}$, $\alpha > \frac{1}{\sqrt{3}}$, the plots of T versus r_+ are shown in Figs. 9 and 10 by considering $\alpha = \beta$ and $\alpha \neq \beta$, respectively. The plots show that, for a suitably fixed parameters, there are two points at which the extreme black holes can occur. We la-

bel them by r_{1ext} and r_{2ext} and suppose that $r_{1ext} < r_{2ext}$. The black holes with the horizon radius in the range $r_{1ext} < r_+ < r_{2ext}$, having positive temperature, are known as the physical black holes. The un-physical black holes, with the negative temperature, occur in the ranges $r_+ < r_{1ext}$ and $r_+ > r_{2ext}$.

The extreme black holes with $\beta = 1$, $\alpha > 0$ occur at the real roots of Eq. (3.4). For the cases $\beta = \alpha$ and $\beta \neq \alpha$, we have shown the plots of T versus r_+ in Figs. 11 and 12, respectively. The point $r_+ = r_{3ext}$ is the horizon radius of the extreme black holes. The physical and un-physical black holes can exist for $r_+ > r_{3ext}$ and $r_+ < r_{3ext}$, respectively.

The other important thermodynamic quantity is the black hole entropy. As a pure geometrical quantity, it can be obtained making use of the Hawking–Bekenstein entropy-area law. According to this nearly universal law, black hole entropy is equal to one-fourth of the black hole horizon area. Thus we have

$$S = \frac{A}{4} = \frac{\pi r_+^2}{g^2(\varepsilon)} (R(r_+))^2 = \frac{\pi b^2}{g^2(\varepsilon)} \left(\frac{b}{r_+} \right)^{2\beta\gamma - 2}, \tag{3.5}$$

which is compatible with that of Reissner–Nordström-A(dS) black holes in the infrared limit of the solutions and in the absence of dilatonic field.

Now, we obtain the black hole's electric potential on the horizon by utilizing the following standard relation [42,43]

$$\Phi = A_\mu \chi^\mu |_{reference} - A_\mu \chi^\mu |_{r=r_+}, \tag{3.6}$$

where, $\chi = C\partial_t$ is the null generator of the horizon and C is an arbitrary constant to be determined. Noting Eqs. (2.14) and (3.6), we have

$$\Phi = \frac{Cq}{B-1} r_+^{1-B}. \tag{3.7}$$

The black hole electric charge Q, as an important conserved quantity, can be obtained in terms of the integration constant q. To do so, one can calculate the total electric flux measured by an observer located at infinity with respect to the horizon (i.e. $r \to \infty$). It is related to the total electric charge of the black hole through the Gauss's electric law which is written in the following form [44, 45]

$$Q = \frac{1}{4\pi} \int r^2 [R(r)]^2 \mathcal{L}'(\mathcal{F}, \phi) F_{\mu\nu} n^\mu u^\nu d\Omega. \tag{3.8}$$

Here, prime means derivative with respect to $\mathcal{F}$, n^μ and u^ν are, in order, the unit timelike and spacelike normals to the hypersurface of radius r. Now, making use of Eqs. (2.14) and (3.8) after some simple calculations we arrived at [23]

$$Q = \frac{qf(\varepsilon)}{g(\varepsilon)b^{B-2}}. \tag{3.9}$$

It reduces to the charge of dilaton black holes when the infrared limit is taken [34].

The other conserved quantity to be calculated is the black hole mass. As mentioned before, it can be obtained in terms of the mass parameter m. Since the asymptotical behavior of the solutions obtained here are not A(dS), we must use the method proposed originally by Brown and York. Based on the Brown and York mass proposal [46–48], known as the subtraction method, if the metric of the spherically symmetric space–time is written in the form,

$$ds^2 = -F^2(r)dt^2 + \frac{dr^2}{G^2(r)} + r^2 d\Omega_2^2, \tag{3.10}$$

and the matter field contains no derivative of the metric, the quasilocal black hole mass can be obtained as

$$M = \lim_{r \to \infty} rF(r) [G(r_0) - G(r)], \tag{3.11}$$

where, $G(r_0)$ is an arbitrary function which determines the zero of the energy for a background spacetime and r is the radius of the spacelike hypersurface boundary [48,49]. It is a matter of calculation to show that the total mass of the new charged rainbow black holes, introduced here, can be obtained as [23,33]

$$M = \frac{mb^{2\beta\gamma}}{2f(\varepsilon)g(\varepsilon)(1 + \beta^2)}, \tag{3.12}$$

which is compatible with the mass of the charged dilaton black holes if we take its infrared limit [34,49].

Now, we are in the position to check the validity of the first law of black hole thermodynamics. To do so, we calculate the intensive thermodynamical quantities from the thermodynamical methods and compare them with those obtained from geometrical methods, up to now. Therefore, it is necessary to obtain the mass of the black holes as a function of the extensive quantities S and Q, through a Smarr-type mass formula.

Regarding Eqs. (3.9) and (3.12) and making use of the fact that the black hole horizon radiuses are the real roots of the relation $U(r_+) = 0$, we arrived at the following Smarr-type mass formula

$$M(r_+, Q) =$$

$$\begin{cases} \frac{b}{2f(\varepsilon)g(\varepsilon)(1-\beta^2)} \left[\frac{r_+}{b} - \frac{\Lambda b^2(1-\beta^4)}{g^2(\varepsilon)(3-\beta^2)} \left(\frac{b}{r_+} \right)^{4\beta\gamma - 3} \right. \\ \left. + \frac{Q^2 g^2(\varepsilon)(1-\beta^2)P(\beta)}{(B-1)b^2} \left(\frac{b}{r_+} \right)^{B-1} \right], \quad \beta \neq 1, \sqrt{3}, \\ -\frac{b}{4f(\varepsilon)g(\varepsilon)} \left[\frac{r_+}{b} + \frac{2\Lambda b^2}{g^2(\varepsilon)} \ln \left(\frac{r_+}{b} \right) \right. \\ \left. - \frac{4g^2(\varepsilon)Q^2 P(\beta=\sqrt{3})}{(\sqrt{3}\alpha-1)b^2} \left(\frac{b}{r_+} \right)^{\frac{1}{2}(\sqrt{3}\alpha-1)} \right], \quad \beta = \sqrt{3}, \alpha > \frac{1}{\sqrt{3}}, \\ \frac{b}{2f(\varepsilon)g(\varepsilon)} \left\{ \left[2 - \frac{\Lambda b^2}{g^2(\varepsilon)} - \frac{Q^2 g^2(\varepsilon)}{b^2} (\frac{\alpha-1}{\alpha+1}) + \ln \left(\frac{b}{r_+} \right) \right] \left(\frac{r_+}{b} \right) \right. \\ \left. + \frac{2Q^2 g^2(\varepsilon)}{\alpha(\alpha+1)b^2} \left(\frac{b}{r_+} \right)^\alpha \right\}, \quad \beta = 1, \alpha > 0. \end{cases} \tag{3.13}$$

In the infrared limit (i.e. $f(\varepsilon) = 1 = g(\varepsilon)$) Eq. (3.13) reduces to the corresponding relation in ref. [34].

Now, making use of Eq. (3.13), it is easy to show that

$$\left(\frac{\partial M}{\partial S} \right)_Q = \left(\frac{\partial M}{\partial r_+} \right)_Q \left(\frac{\partial S}{\partial r_+} \right)_Q^{-1} = T \quad \text{and} \quad \left(\frac{\partial M}{\partial Q} \right)_S = \Phi, \tag{3.14}$$

provided that the constant coefficient C be fixed as $C = P(\beta)$ for both $\beta = \sqrt{3}$, $\beta \neq \sqrt{3}$, 1 cases. Also, they are fulfilled for the case $\beta = 1$, if we set $r_+ = b$, $C = 2 - \alpha$. It is notable that we have $C = 1$, if one sets $\beta = \alpha$. It means that, although the thermodynamic quantities are affected by the rainbow functions, the first law of black hole thermodynamics remains valid for all of the three new charged dilaton black hole solutions, in the following form

$$dM(S, Q) = TdS + \Phi dQ, \tag{3.15}$$

where T and Φ are known as the thermodynamical intensive parameters conjugate to the extensive parameters S and Q, respectively.

4. Thermal stability of the new rainbow black holes

The thermodynamic stability or phase transition of a system can be considered by analyzing the sign of the heat capacity C_Q
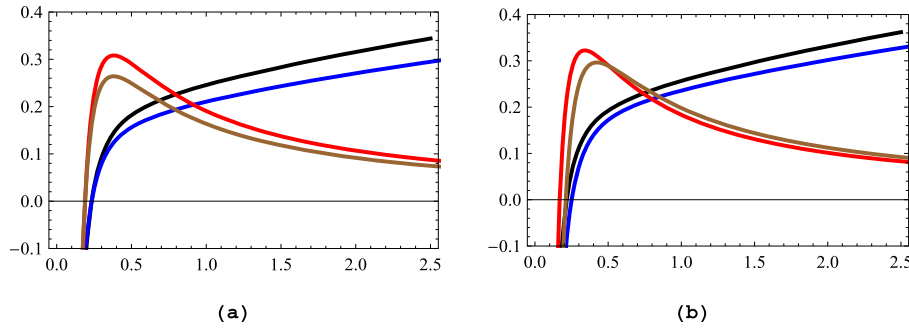
(a)   **(b)**

Fig. 7. T and $\left(\partial^2 M/\partial S^2\right)_Q$ versus r_+ for $Q = 0.5$, $M = 2$, $\Lambda = -3$, $b = 1.6$, $\alpha = \beta = 0.6$, Eqs. (3.1) and (4.2). (a): $g(\varepsilon) = 0.85$, $[0.5T : f(\varepsilon) = 1.2$ (black), 1.4 (blue)] and $[10\left(\partial^2 M/\partial S^2\right)_Q : f(\varepsilon) = 1.2$ (red), 1.4 (brown)]. (b): $f(\varepsilon) = 1.2$, $[0.5T : g(\varepsilon) = 0.8$ (black), 0.9 (blue)] and $[10\left(\partial^2 M/\partial S^2\right)_Q : g(\varepsilon) = 0.8$ (red), 0.9 (brown)].

at constant electric charge. The black hole heat capacity, calculated in the fixed black hole's charge, is defined as

$$C_Q = T\left(\frac{\partial S}{\partial T}\right)_Q = T\left(\frac{\partial^2 M}{\partial S^2}\right)_Q^{-1}. \quad (4.1)$$

The last step in Eq. (4.1) comes from the fact that $T = (\partial M/\partial S)_Q$. From the view point of canonical ensemble method positivity of the black hole heat capacity is a necessary condition for the system to be locally stable. The local stability of a system will be ensured only if there exists a range of the horizon radius for which the quantities T and $\left(\partial^2 M/\partial S^2\right)_Q$ are both positives. The unstable black holes undergo phase transitions to be stabilized. Type-1 phase transition occurs at the points where the black hole heat capacity vanishes. It means that the unstable black holes undergo type-1 phase transition at the real root(s) of $T = 0$. Note that the numerator of the black hole heat capacity is the black hole temperature which is given by Eq. (3.1). In addition, unstable black holes undergo type-2 phase transition at the points where the black hole heat capacity diverges. Therefore, the points of type-2 phase transition are the real root(s) of $\left(\partial^2 M/\partial S^2\right)_Q = 0$ [42,43]. Regarding these issues, we proceed to analyzing the thermal stability or phase transition of our new rainbow black hole solutions, separately.

4.1. Black holes with $\beta \neq 1$, $\sqrt{3}$

To perform a thermal stability analysis we need to calculate the black hole heat capacity. Making use of Eq. (3.13), we calculated the denominator of the black hole heat capacity in the following form

$$\left(\frac{\partial^2 M}{\partial S^2}\right)_Q = \frac{-g^3(\varepsilon)(1 + \beta^2)}{8\pi^2 f(\varepsilon)b^3}\left(\frac{b}{r_+}\right)^{3-4\beta\gamma}$$
$$\times\left[1 - \frac{\Lambda b^2(\beta^2 - 1)}{g^2(\varepsilon)}\left(\frac{b}{r_+}\right)^{4\beta\gamma-2}\right.$$
$$\left. - f^2(\varepsilon)q^2 P_1(\beta)\left(\frac{b}{r_+}\right)^B\right], \quad (4.2)$$

where

$$P_1(\beta) = \frac{(1 + \beta^2)(B - 2\beta\gamma + 1)P(\beta)}{b^{2(B-1)}}.$$

The plots of $\left(\partial^2 M/\partial S^2\right)_Q$ versus r_+, for different values of rainbow functions, are shown in Figs. 7 and 8 for $\beta = \alpha$ and $\beta \neq \alpha$ cases, respectively. As it is clear from Fig. 7, black holes with $\beta = \alpha$ undergo type-1 phase transition at $r_+ = r_{ext}$ where the black hole

heat capacity vanishes. Also, the black hole heat capacity diverges at the point $r_+ = r_1$. This is a point of type-2 phase transition. This class of black holes are locally stable if their horizon radius be in the range $r_+ > r_{ext}$.

The plots of Fig. 8 show that the denominator of the black hole heat capacity (i.e. $\left(\partial^2 M/\partial S^2\right)_Q$) is positive and no type-2 phase transition takes place. Also, they show that the temperature (or numerator of the heat capacity) vanishes at the point $r_+ = r_{ext}$. This point is the point of type-1 phase transition. The black holes with the horizon radius r_+, greater than r_{ext} have positive heat capacity and are locally stable.

4.2. Black holes with $\beta = \sqrt{3}$, $\alpha > \frac{1}{\sqrt{3}}$

It is matter of calculation to show that the denominator of the black hole capacity is given by

$$\left(\frac{\partial^2 M}{\partial S^2}\right)_Q = \frac{-g^3(\varepsilon)}{2\pi^2 f(\varepsilon)b^3}\left[1 - \frac{2\Lambda b^2}{g^2(\varepsilon)}\left(\frac{b}{r_+}\right)\right.$$
$$\left. - f^2(\varepsilon)q^2 P_1(\beta = \sqrt{3})\left(\frac{b}{r_+}\right)^{\frac{1}{2}(\sqrt{3}\alpha+1)}\right]. \quad (4.3)$$

It is well-known that the points of type-2 phase transition are characterized by the real roots of Eq. (4.3). In order to explore the existence and number of these roots, we have plotted $\left(\partial^2 M/\partial S^2\right)_Q$ versus r_+ for both of $\beta = \alpha$ and $\beta \neq \alpha$ cases in Figs. 9 and 10, separately. The plots show that the denominator of the black hole heat capacity vanishes at $r_+ = r_2$ and the black hole heat capacity diverges at this point for both of $\beta = \alpha$ and $\beta \neq \alpha$ cases. Thus there is a point of type-2 phase transition located at $r_+ = r_2$. The numerator of black hole heat capacity (i.e. T) vanishes at the points $r_+ = r_{1\,ext}$ and $r_+ = r_{2\,ext}$ with $r_{1\,ext} < r_{2\,ext}$. It means that the type-1 phase transition takes place at the points $r_+ = r_{1\,ext}$ and $r_+ = r_{2\,ext}$. The heat capacity of the black holes with horizon radius in the range $r_{1\,ext} < r_+ < r_2$ is positive and they are locally stable.

4.3. Black holes with $\beta = 1$, $\alpha > 0$

Starting from Eq. (3.13), the denominator of the black hole heat capacity can be calculated. It can be written in the following form:

$$\left(\frac{\partial^2 M}{\partial S^2}\right)_Q = \frac{-g^3(\varepsilon)}{2\pi^2 f(\varepsilon)b^2 r_+}\left[1 - \frac{2f^2(\varepsilon)q^2}{b^{2\alpha}}\left(\frac{b}{r_+}\right)^{\alpha+1}\right]. \quad (4.4)$$

As it is shown in Figs. 11 and 12, the heat capacity of the black holes with $\beta = 1$, vanishes at $r_+ = r_{3\,ext}$, where the extreme black holes occur. The type-1 phase transition takes place at this point
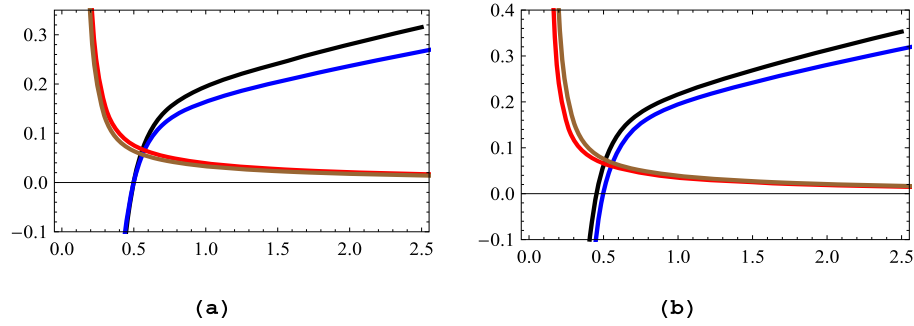
Fig. 8. T and $\left(\partial^2 M/\partial S^2\right)_Q$ versus r_+ for $Q=0.5$, $M=2$, $\Lambda=-3$, $b=2$, $\alpha=2.5$, $\beta=0.5$, Eqs. (3.1) and (4.2). (a): $g(\varepsilon)=0.85$, $[0.5T: f(\varepsilon)=1.35$ (black), 1.6 (blue)] and $[2\left(\partial^2 M/\partial S^2\right)_Q: f(\varepsilon)=1.35$ (red), 1.6 (brown)]. (b): $f(\varepsilon)=1.35$, $[0.5T: g(\varepsilon)=0.75$ (black), 0.85 (blue)] and $[2\left(\partial^2 M/\partial S^2\right)_Q: g(\varepsilon)=0.75$ (red), 0.85 (brown)].
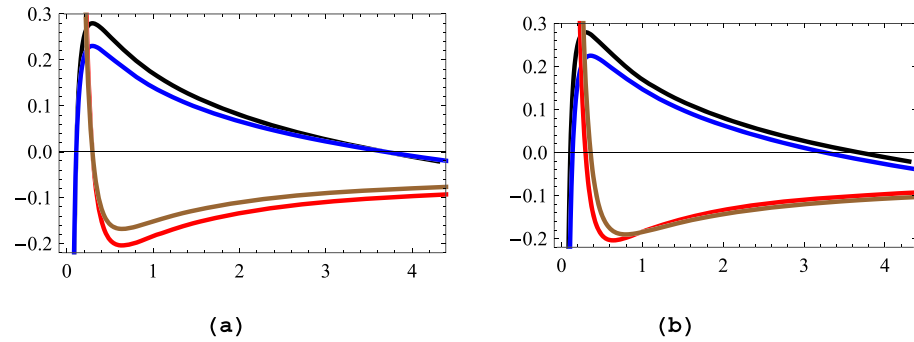

Fig. 9. T and $\left(\partial^2 M/\partial S^2\right)_Q$ versus r_+ for $Q=0.5$, $\Lambda=-3$, $b=0.8$, $\alpha=\beta=\sqrt{3}$, Eqs. (3.1) and (4.3). (a): $g(\varepsilon)=0.9$, $[0.5T: f(\varepsilon)=1.4$ (black), 1.7 (blue)] and $[\left(\partial^2 M/\partial S^2\right)_Q: f(\varepsilon)=1.4$ (red), 1.7 (brown)]. (b): $f(\varepsilon)=1.4$, $[0.5T: g(\varepsilon)=0.9$ (black), 0.95 (blue)] and $[\left(\partial^2 M/\partial S^2\right)_Q: g(\varepsilon)=0.9$ (red), 0.95 (brown)].
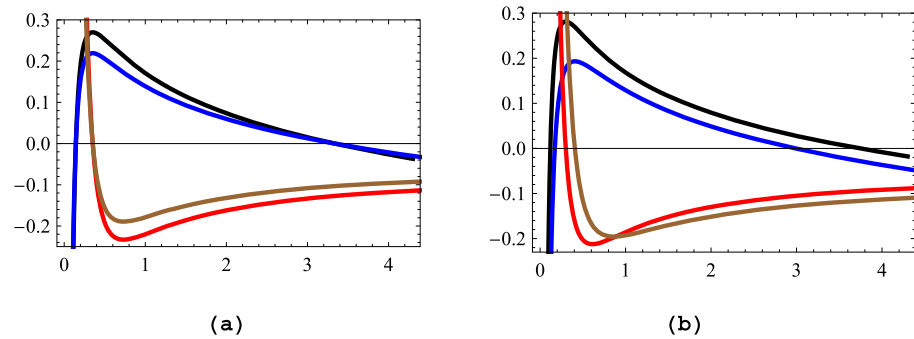

Fig. 10. T and $\left(\partial^2 M/\partial S^2\right)_Q$ versus r_+ for $Q=0.5$, $\Lambda=-3$, $b=0.8$, $\alpha=2$, $\beta=\sqrt{3}$, Eqs. (3.1) and (4.3). (a): $g(\varepsilon)=0.95$, $[0.5T: f(\varepsilon)=1.3$ (black), 1.6 (blue)] and $[\left(\partial^2 M/\partial S^2\right)_Q: f(\varepsilon)=1.3$ (red), 1.6 (brown)]. (b): $f(\varepsilon)=1.5$, $[0.5T: g(\varepsilon)=0.9$ (black), 1 (blue)] and $[\left(\partial^2 M/\partial S^2\right)_Q: g(\varepsilon)=0.9$ (red), 1 (brown)].
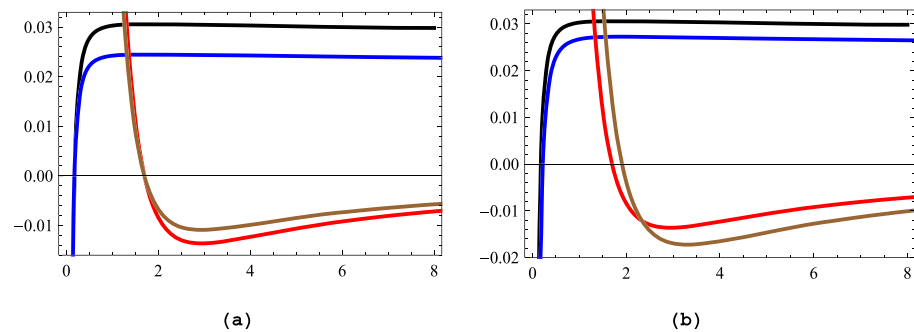

Fig. 11. T and $\left(\partial^2 M/\partial S^2\right)_Q$ versus r_+ for $Q=1.5$, $\Lambda=-3$, $b=3$, $\alpha=\beta=1$, Eqs. (3.1) and (4.4). (a): $g(\varepsilon)=0.8$, $[0.02T: f(\varepsilon)=1.2$ (black), 1.5 (blue)] and $[25\left(\partial^2 M/\partial S^2\right)_Q: f(\varepsilon)=1.2$ (red), 1.5 (brown)]. (b): $f(\varepsilon)=1.2$, $[0.02T: g(\varepsilon)=0.8$ (black), 0.9 (blue)] and $[\left(25\partial^2 M/\partial S^2\right)_Q: g(\varepsilon)=0.8$ (red), 0.9 (brown)].
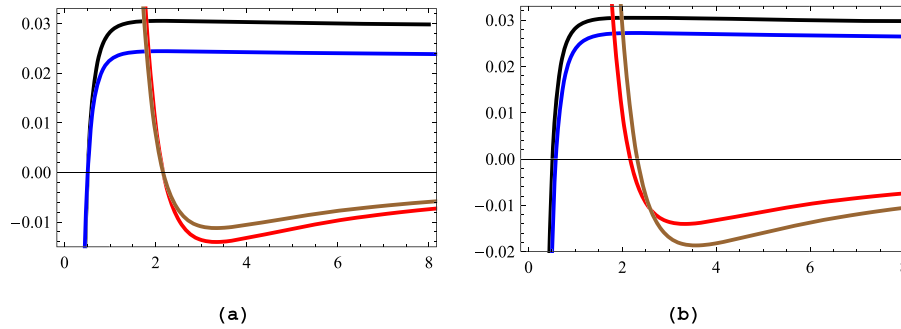
Fig. 12. T and $\left(\partial^2 M/\partial S^2\right)_Q$ versus r_+ for $Q = 1.5$, $\Lambda = -3$, $b = 3$, $\alpha = 2.5$, $\beta = 1$, Eqs. (3.1) and (4.4). (a): $g(\varepsilon) = 0.8$, $[0.02T : f(\varepsilon) = 1.2$ (black), 1.5 (blue)] and $[25\left(\partial^2 M/\partial S^2\right)_Q : f(\varepsilon) = 1.2$ (red), 1.5 (brown)]. (b): $f(\varepsilon) = 1.2$, $[0.02T : g(\varepsilon) = 0.8$ (black), 0.9 (blue)] and $[25\left(\partial^2 M/\partial S^2\right)_Q : g(\varepsilon) = 0.8$ (red), 0.9 (brown)].

for both of the $\alpha = \beta$ and $\alpha \neq \beta$ cases. Also, the denominator of the black hole heat capacity vanishes at $r_+ = r_3$. Thus, the black hole heat capacity diverges at $r_+ = r_3$ and it is a point of type-2 phase transition. This class of new black holes with $\alpha = \beta$ and $\alpha \neq \beta$ cases are locally stable if their horizon radiuses are in the range $r_{3\ ext} < r_+ < r_3$.

5. Conclusion

In the present work, we studied the thermodynamics and thermal stability of the charged dilaton black holes in gravity's rainbow. By varying the related four-dimensional action the equations of coupled scalar, vector and tensor fields have been obtained in the presence of the rainbow functions. We introduced a four-dimensional spherically symmetric energy dependent geometry and solved the coupled field equations. As the result we obtained two sets of electromagnetic solutions. One is the Coulomb's inverse square electric field and the other is interpreted as a modified Coulomb's electric field. The scalar field equation has been solved and the solution has been written as the linear combination of three Liouville-type potentials. Three new classes of charged dilaton black holes have been obtained as the exact solutions to the Einstein–Maxwell-dilaton theory in the rainbow gravity. The asymptotic behavior of the solutions are neither flat nor A(dS). Also, with the properly fixed parameters, the solutions show the two horizon, extreme and naked singularity black holes (Figs. 1–6). Existence of the horizons together with the singular Ricci scalars at $r = 0$ are in favor of the black hole interpretation of the solutions.

In order to investigate the thermodynamic properties of the charged dilaton black hole solutions, obtained in this work, we calculated the thermodynamic quantities (i.e. temperature, entropy and electric potential) and the conserved quantities (i.e. charge and mass) related to the new rainbow black holes. We showed that, for the properly fixed parameters, the extreme black holes having zero temperature can occur.

For the black holes with $\beta \neq 1$, $\sqrt{3}$ the black hole temperature vanishes at $r_+ = r_{ext}$. The physical black holes, having positive temperature, occur for $r_+ > r_{ext}$ and the un-physical black holes with negative temperature are those have a horizon radius less than $r_+ = r_{ext}$. The plots of T versus r_+ for the cases $\alpha = \beta$ and $\alpha \neq \beta$ are shown in Figs. 7 and 8, respectively.

The temperature of the black holes corresponding to $\beta = \sqrt{3}$, vanishes at the points $r_+ = r_{1ext}$ and $r_+ = r_{2ext}$ such that $r_{1ext} < r_{2ext}$. This kind of black holes are physically reasonable provided that their horizon radius be in the range $r_{1ext} < r_+ < r_{2ext}$. The un-physical black holes (i.e. the black holes with negative temperature) appear for $r_+ < r_{1ext}$ and $r_+ > r_{2ext}$. We have plotted T versus r_+ in Figs. 9 and 10 for $\alpha = \beta$ and $\alpha \neq \beta$ cases, respectively.

The horizon of the extreme black holes with $\beta = 1$ is located at $r_+ = r_{3ext}$. It is the real root of equation (3.4). As shown in Figs. 11 and 12, the horizon radii of the physical and un-physical black holes satisfy the relations $r_+ > r_{3ext}$ and $r_+ < r_{3ext}$, respectively.

We derived a Smarr-type mass formula which shows the black hole mass as a function of black hole charge Q and entropy S named as the extensive thermodynamical parameters. Making use of the Smarr mass formula we proved that, even if the thermodynamic quantities are affected by the rainbow functions, the thermodynamical first law is still valid for either of the new black hole solutions.

Finally, we have performed a thermal stability analysis for the new dilaton black holes obtained here. We have analyzed the stability of our new black hole solutions making use of the canonical ensemble method. By calculating the black hole heat capacity and noting its signature we have determined the points of type-1 and type-2 phase transitions as well as the ranges at which the black holes are locally stable, precisely. It has been found that: (i) For the black holes with $\beta \neq 1$, $\sqrt{3}$, if we set $\alpha = \beta$, there is a point of type-1 phase transition located at the vanishing point of the black hole temperature. The point of type-2 phase transition is located at $r_+ = r_1$ where the denominator of the black hole heat capacity vanishes. This kind of black holes are locally stable if their horizon radius is in the range $r_+ > r_1$ where the black hole heat capacity is positive (see Fig. 7). As it is shown in Fig. 8, by setting $\alpha \neq \beta$ it is possible to fix the parameters such that the denominator of the black hole heat capacity be positive valued. Thus, there is no point of type-2 phase transition. The black holes undergo type-1 phase transition at the vanishing point of the black hole temperature located at $r_+ = r_{ext}$. They are locally stable if their horizon radius is greater than r_{ext}. (ii) The black holes corresponding to $\beta = \sqrt{3}$ undergo type-1 phase transition at the points $r_+ = r_{1ext}$ and $r_+ = r_{2ext}$. There is a point of type-2 phase transition located at the divergent point of the black hole heat capacity located at $r_+ = r_2$. These kinds of black holes with the horizon radius in the range $r_{1\ ext} < r_+ < r_2$ are locally stable. These facts can be seen in the plots of Figs. 9 and 10 for the $\alpha = \beta$ and $\alpha \neq \beta$ cases, respectively. (iii) The black holes with $\beta = 1$ undergo type-1 phase transition at the vanishing point of the black hole heat capacity located at $r_+ = r_{3ext}$. There is a point of type-2 phase transition located at $r_+ = r_3$ where the black hole heat capacity diverges. These kinds of black holes are locally stable provided that their horizon radiuses are in the range $r_{ext} < r_+ < r_3$. Figs. 11 and 12 show the numerator and denominator of the black hole heat capacity for the cases $\alpha = \beta$ and $\alpha \neq \beta$ cases, respectively.

Acknowledgements

References

[1] V.A. Kostelecky, S. Samuel, Phys. Rev. D 39 (1989) 683.
[2] D. Amati, M. Ciafaloni, G. Veneziano, Phys. Lett. B 197 (1987) 81.
[3] R. Gambini, J. Pullin, Phys. Rev. D 59 (1999) 124021.
[4] G. Amelino-Camelia, J.R. Ellis, N.E. Mavromatos, D.V. Nanopoulos, S. Sarkar, Nature 393 (1998) 763.
[5] P. Horava, Phys. Rev. Lett. 102 (2009) 161301.
[6] M. Faizal, J. Phys. A 44 (2011) 402001.
[7] M.R. Douglas, N.A. Nekrasov, Rev. Mod. Phys. 73 (2001) 977.
[8] F. Girelli, E.R. Livine, D. Oriti, Nucl. Phys. B 708 (2005) 411.
[9] J. Magueijo, L. Smolin, Phys. Rev. Lett. 88 (2002) 190403.
[10] J. Magueijo, L. Smolin, Phys. Rev. D 67 (2003) 044017.
[11] G. Amelino-Camelia, Int. J. Mod. Phys. D 11 (2002) 1643.
[12] R. Garattini, E.N. Saridakis, Int. J. Mod. Phys. D 25 (2016) 1650101.
[13] A.F. Ali, Phys. Rev. D 89 (2014) 104040.
[14] E.J. Son, W. Kim, Mod. Phys. Lett. A 30 (2015) 1550178.
[15] J. Magueijo, L. Smolin, Phys. Rev. D 67 (2003) 044017.
[16] J. Magueijo, L. Smolin, Class. Quantum Gravity 21 (2004) 1725.
[17] J. Magueijo, L. Smolin, Phys. Rev. D 71 (2005) 026010.
[18] M. Dehghani, Phys. Lett. B 777 (2018) 351.
[19] Z-W. Feng, S-Z. Yang, Phys. Lett. B 772 (2017) 737.
[20] U. Jacob, F. Mercati, G. Amelino-Camelia, T. Piran, Phys. Rev. D 82 (2010) 084021.
[21] G. Amelino-Camelia, Living Rev. Relativ. 16 (2013) 5.
[22] Y. Ling, X. Li, H. Zhang, Mod. Phys. Lett. A 36 (2007) 2749.
[23] S.H. Hendi, S. Panahiyan, B. Eslam Panah, M. Momennia, Eur. Phys. J. C 76 (2016) 150.
[24] S.H. Hendi, B. Eslam Panah, S. Panahiyan, M. Momennia, Eur. Phys. J. C 77 (2017) 647.
[25] S. Alsaleh, Int. J. Mod. Phys. A 32 (2017) 1750076.
[26] S.H. Hendi, M. Faizal, Phys. Rev. D 92 (2015) 044027.
[27] S.H. Hendi, S. Panahiyan, B. Eslam Panah, M. Faizal, M. Momennia, Phys. Rev. D 94 (2016) 044028.
[28] S.H. Hendi, S. Panahiyan, S. Upadhyay, B. Eslam, Phys. Rev. D 95 (2017) 084036.
[29] S.H. Hendi, B. Eslam Panah, S. Panahiyan, Phys. Lett. B 769 (2017) 191.
[30] A.F. Ali, M. Faizal, M.M. Khalil, Nucl. Phys. B 894 (2015) 341.
[31] A.F. Ali, Phys. Rev. D 89 (2014) 104040.
[32] S.H. Hendi, M. Momennia, B. Eslam Panah, M. Faizal, Astrophys. J. 827 (2016) 153.
[33] M. Dehghani, Phys. Lett. B 781 (2018) 553.
[34] M. Dehghani, Int. J. Mod. Phys. D 27 (2018) 1850073.
[35] A. Sheykhi, S. Hajkhlili, Phys. Rev. D 89 (2014) 104019.
[36] M. Dehghani, Phys. Rev. D 96 (2017) 044014.
[37] M. Dehghani, Phys. Lett. B 773 (2017) 105.
[38] M.H. Dehghani, A. Sheykhi, Z. Dayyani, Phys. Rev. D 93 (2016) 024022.
[39] Z. Dayyani, A. Sheykhi, M.H. Dehghani, Phys. Rev. D 95 (2017) 084004.
[40] M. Dehghani, Phys. Rev. D 97 (2018) 044030.
[41] M. Dehghani, S.F. Hamidi, Phys. Rev. D 96 (2017) 104017.
[42] M. Kord Zangeneh, M.H. Dehghani, A. Sheykhi, Phys. Rev. D 92 (2015) 104035.
[43] M. Dehghani, Phys. Rev. D 94 (2016) 104071.
[44] M. Dehghani, Phys. Rev. D 98 (2018) 044008.
[45] M. Dehghani, S.F. Hamidi, Phys. Rev. D 96 (2017) 044025.
[46] J.D. Brown, J. York, Phys. Rev. D 47 (1993) 1407.
[47] J.D. Brown, J. Creighton, R.B. Mann, Phys. Rev. D 50 (1994) 6394.
[48] K.C.K. Chan, J.H. Home, R.B. Mann, Nucl. Phys. B 447 (1995) 441.
[49] A. Sheykhi, A. Kazemi, Phys. Rev. D 90 (2014) 044028.